

# STUDY ON DAMAGES OF LAVER AQUACULTURE FACILITIES IN TOKYO BAY FROM 2011 TOHOKU EARTHQUAKE TSUNAMI

D.P.C. Laknath<sup>1</sup>, Takahide Honda<sup>2</sup>, Kazunori Ito<sup>3</sup>, Jun Sasaki<sup>4</sup>, Yuriko Takayama<sup>5</sup>  
and Yukinobu Oda<sup>6</sup>

<sup>1</sup>Technology Center, Taisei Corporation, laknath@pub.taisei.co.jp

<sup>2</sup>Technology Center, Taisei Corporation, hndtkh01@pub.taisei.co.jp

<sup>3</sup>Technology Center, Taisei Corporation, kazunori.ito@sakura.taisei.co.jp

<sup>4</sup>Faculty of Urban Innovation, Yokohama National University, jsasaki@estuarine.jp

<sup>5</sup>Technology Center, Taisei Corporation, yuriko.takayama@sakura.taisei.co.jp

<sup>6</sup>Technology Center, Taisei Corporation, od-ykn00@pub.taisei.co.jp

In scientific literature, damage processes of laver aquaculture facilities (*Nori-Hibi*) under the tsunami flow have not been dealt with in depth so far. Hence, as an initiative step to explore the possible failure mechanisms and resultant drifting processes of the *Nori-Hibi* compartments, *Nori-Hibi* damages in Tokyo Bay, caused by 2011 Tohoku Earthquake Tsunami was studied with numerical simulation. After estimating possible damages in study area based on reproduced hydrodynamic conditions and resultant external forces, different failure modes were assessed to understand the failure mechanism. Due to the complexity of the selected failure modes, driftage simulation was performed only for the "breakage of supporting pole" failure mode. Field investigated damage intensities of the *Nori-Hibi* compartments in the Futtsu cape and Banzu tidal flat areas can be qualitatively explained through this failure mode.

**Key Words:** *Nori-Hibi*, tsunami damages, failure modes, Delft3D, driftage simulation model

## 1. INTRODUCTION

2011 Tohoku Earthquake Tsunami caused significant damages to the laver aquaculture farming in Tokyo Bay. Since there is a possibility of recurrence of tsunamis in the same region, further study about the intensity of past damages and damage mechanisms of the laver aquaculture facilities (here after *Nori-Hibi* sets) are important to estimate the future damages. In recent studies, Sasaki *et al.* (2012) investigated damages due to the tsunami on *Nori-Hibi* farming in eastern part of the bay. Their study identified a positive correlation between the scale of damages and the hydraulic resistance on laver nets. However, in the scientific literature, damage mechanisms of *Nori-Hibi* sets and driftage under the tsunami flow have not been well revealed because of the shortage of field data. Therefore, for the further understanding of the damage processes, the objectives of the present study are to consider possible failure modes and explain the scale of damages and driftage of *Nori-Hibi* sets in the Futtsu cape and Banzu tidal flat areas in Tokyo Bay (**Fig. 1 (a)**).

## 2. STUDY AREA

*Nori-Hibi* is an aquaculture facility for catching the spores of laver ("*nori*"), and to grow the laver nursery. In early days, laver spores had been collected by planting bamboo or brushwood ("*hibi*") in shallow waters. In 1940s, a traditional farming method was improved to the present one using "fixed nets" (or "pole system") consisting of synthetic material nets and bamboo poles. In this

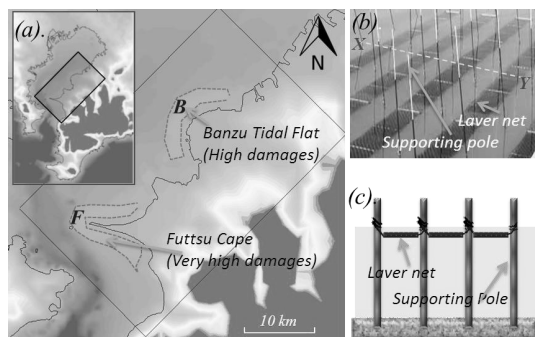


**Fig.1** (a). *Nori-Hibi* sets damaged areas in Tokyo Bay (b). Typical arrangement of the *Nori-Hibi* compartment (c). Sectional view of *Nori-Hibi* compartment across XY.

**Table 1** Damaged details of *Nori-Hibi* sets in Tokyo Bay. (Source: Sasaki *et al.*, 2012)

Location	Description of damage	Damage scale
Banzu tidal flat	<ul style="list-style-type: none"> <li>• <i>Ushigome</i>: 2 sets collapsed</li> <li>• <i>Kaneda</i>: 7 sets destroyed</li> </ul>	<b>High damages</b>
Futtso cape	<ul style="list-style-type: none"> <li>• <i>Futtso fishery cooperative Farming bed</i>: 33 sets destroyed.</li> <li>• <i>Shin-Futtso farming bed</i>: 170 sets were damaged and 116 sets destroyed.</li> </ul>	<b>Very high damages</b>

arrangement, laver aquaculture nets are stretched between supporting poles (bamboos). Supporting poles are fixed to the shallow water bed (Borgese, 1980). Laver nets float on the water surface with the tidal motion (Fig. 1 (b & c)). During the ebb tide period, the nets are exposed periodically to the air.

According to the field survey results of Sasaki *et al.* (2012), identified tsunami damages of *Nori-Hibi* sets in study area are summarized in Table 1, where the details of damage are presented in terms of the number of damaged *Nori-Hibi* sets. Accordingly, the scale of damage for *Nori-Hibi* sets in the Futtso cape area is much higher than that in the Banzu tidal flat area.

### 3. METHODOLOGY

For the detailed understanding of damages on *Nori-Hibi* sets, tsunami induced hydrodynamic characteristics, including flow velocities and water depths were reproduced using Delft3D–Flow hydrodynamic model (Deltares, 2010) for six hours of model period. To evaluate the resistance of *Nori-Hibi* set due to the external forces induced by tsunami flow, effects on idealized *Nori-Hibi* compartment consisting of 4 nets (40 m × 3 m) and 40 supporting poles (32 mm diameter) were considered (Fig. 2). As main horizontal forces on *Nori-Hibi* compartment, hydraulic resistances on laver net ( $F_{Net}$ ) and drag forces on supportive poles ( $F_{Drag}$ ) were considered. According to Yagi *et al.* (2009), laver net resistance force (for single net) was calculated using the following equation.

$$F_{Net} = \frac{1}{2} \rho C_{net} U^2 A \quad (1)$$

where  $\rho$  is the density of sea water,  $U$  is the depth averaged velocity and  $A$  is the surface area of the net. The resistance coefficient of the laver net ( $C_{net}$ ) was taken as 0.02, assuming high quantity of laver at the 2011 tsunami event (Yagi *et al.*, 2009). Further, the total laver net force ( $F_{TNet}$ ) acting on a compartment was calculated by multiplying  $F_{Net}$  by the number of laver nets in the compartment (Fig. 2 (a)). The total drag forces on supporting poles per compartment were calculated based on the "drag law" using the following equation (Schlichting, 1979).

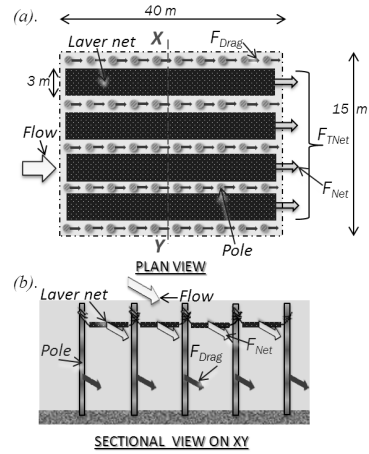


**Fig.2** Typical arrangement of *Nori-Hibi* compartment.

$$F_{Drag} = \frac{1}{2} \rho C_d D h U^2 N \quad (2)$$

where  $C_d$  is the resistance coefficient of a circular cylinder ( $=1.1$ ),  $D$  is the diameter of the supporting pole,  $h$  is the water depth and  $N$  is the number of poles per compartment. In case of vertical direction, buoyancy forces ( $b$ ) on submerged laver nets and self-weight ( $w$ ) of the *Nori-Hibi* set were considered as main forces. In this study, possible failure modes for *Nori-Hibi* compartment were assumed because the real failure mechanism is unknown. Thus, on the basis of combined different external forces, three possible failure modes namely, "breakage of supporting poles", "breakage of ropes" and "pulling out of poles" were defined and tabulated in Table 2. Considering the material properties (e.g. bending strength/shear strength of bamboo, tensile strength of rope) and maximum internal forces developed in the structure (bending and shear stresses), damage modes were further analyzed to find out the threshold values of the parameters at the failure. As shown in Fig. 3, computed hydrodynamic parameters (flow depths and flow velocities) using Delft3D-Flow and criteria developed to initiate the driftage of the drifting objects were used as the

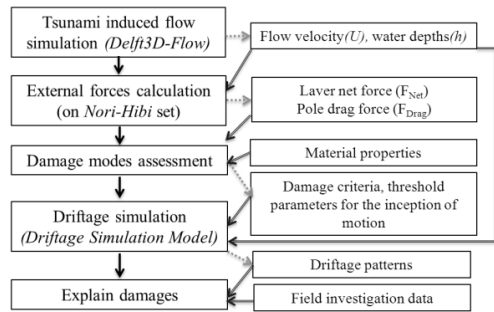


**Fig.3** Sequence of processes and input/ output of each process.

**Table 2** Failure modes of *Nori-Hibi* set.

Failure Mode	Forces			
	$F_{Net}$	$F_{Drag}$	w	b
1. Breakage of supporting poles	○	○	-	-
2. Breakage of ropes	○	-	-	-
3. Pulling out of poles	○	○	○	○

○ = Included, - = Not included

input parameters for the driftage simulation model. This model has been successfully used by Takayama *et al.* (2010) to simulate the driftage paths of Scallop Larva in Lake Saroma. Finally, on the basis of identified driftage pattern, damages on *Nori-Hibi* sets in the study areas were explained.

## 4. RESULTS AND DISCUSSION

### (1) Hydrodynamic characteristics

Fig. 4 shows flow patterns and time varying flow velocities, water depths and external forces calculated for the representative locations for Banzu

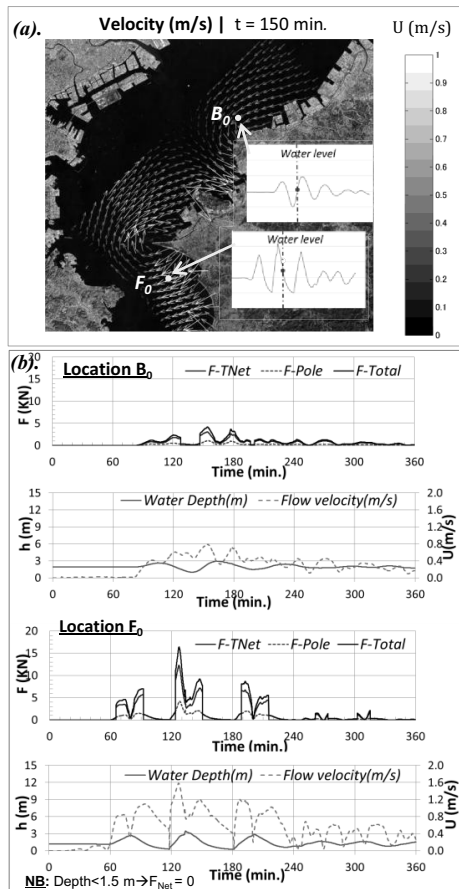


**Fig.4** (a). Depth averaged velocity at 150 min. (b).Variation of external forces (F), flow velocity (U) and flow depth (h) at  $B_0$  and  $F_0$ .

tidal flat and Futtsu cape areas ( $B_0$  and  $F_0$  respectively). As shown in Fig. 4 (a), higher flow velocities are visible in both areas. Since flow velocities are positively correlated with induced horizontal forces, much higher forces and consequently higher damages can be expected in both areas. As clearly shown in Fig. 4 (b), total force exerted on a *Nori-Hibi* compartment in the  $F_0$  area is much higher than in the  $B_0$  area. Therefore, the intensity of damage in the  $F_0$  area could be higher compared to that in  $B_0$  area. Thus, field investigated damages are in agreement with the numerical reproduced results.

### (2) Assessment of various failure modes

#### a) Breakage of supporting poles

Breakage of supporting poles was assessed for both bending and shears failure modes. As a result of exerted horizontal forces ( $F_{Net}$  and  $F_{Drag}$ ), maximum bending moments and shear forces along a bamboo pole were analyzed (Fig. 5). To estimate the horizontal laver net force acting on a single pole, total laver net force on a compartment ( $F_{TNet}$ ) was equally distributed among the number of supporting poles. Since Delft3D simulation results are depth averaged values, velocity distribution of flow currents in vertical direction could not be obtained. Due to the fact that tsunami wavelength is far longer than normal waves, approximation under "very shallow water wave condition" can be adopted. Under this condition, horizontal velocity distribution along the depth does not change much. Therefore, drag force along the pole can be assumed as uniform. Considering horizontal loading conditions on supporting pole, maximum bending forces ( $M_{Max}$ ) and maximum shear force ( $V_{Max}$ ) were calculated. Further, internally developed forces such as maximum bending stress ( $f_{max}$ ) and maximum shear stress ( $\tau_{max}$ ) across the critical cross section of the bamboo pole were calculated by using theory of bending and shear. Since size and material properties of bamboo pole are unknown values, threshold velocities were calculated for three criteria (for bending failure: BF1, BF2, BF3 criteria and corresponding SF1, SF2, SF3 criteria for shear failure). For each criterion, selected outer and inner

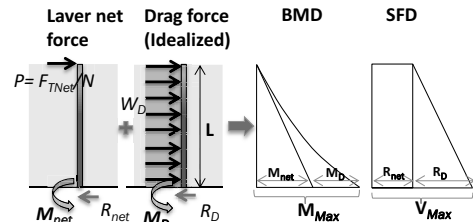


**Fig.5** External horizontal forces, bending moment (BMD) and shear force diagrams (SFD) for supporting pole.

**Table 3** Details of bending and shear failure criteria.

Criteria	Type	$D_0$ , mm	$D_1$ , mm	$f_s$ N/mm <sup>2</sup>	$\tau_s$ N/mm <sup>2</sup>
BF1	Bending	32	20	25	-
BF2	Bending	50	40	84	-
BF3	Bending	100	90	84	-
SF1	Shear	32	20	-	7.5
SF2	Shear	50	40	-	7.5
SF3	Shear	100	90	-	7.5

diameters ( $D_0$  and  $D_1$ ), maximum bending ( $f_s$ ) and shear ( $\tau_s$ ) strengths of the bamboo pole are presented in **Table 3**. Dimensions and strength properties of the bamboo were selected in order to represent the weak and strong properties of the material. Further, to estimate the threshold velocity against the shear failure, lower limit of the shear strength of bamboo (7.5 N/mm<sup>2</sup>) was considered (Janssen, 1981). Accordingly, minimum flow velocities required for the failure of bamboo for both bending and shear modes were calculated for each criterion at different depths. As highlighted in **Fig. 6**, bending failure is always dominant for bamboo pole because minimum flow velocities require for the bending failure are much less than similar size shear failure case (e.g. BF1 and SF1). Hence, bending failure governs the damages of bamboo poles. Further, calculated threshold velocities for the bending and shear failure were compared with the flow velocities representing normal (*Case-I*:  $H_s=1$  m,  $T_p=12$  sec) and extreme (*Case-II*:  $H_s=3$  m,  $T_p=12$  sec) wave conditions. As illustrated in **Fig. 6**, minimum velocities require for the bending failure (velocities between BF1 and BF3) are lower than the extreme wave condition velocities (*Case-II*). This result implies the higher tendency of damages (due to bending failure) for the supporting poles under the extreme wave conditions. On the other hand, compared with the flow velocities corresponding to the normal wave conditions, calculated threshold velocities for the bending failure (BF1~BF3) are expected to be higher than the normal wave condition (*Case-I*). However, as shown in **Fig. 6**, BF1 values are lower than the normal wave condition (*Case-I*).

According to this result, it is clear that, estimated threshold velocities for the bending failure

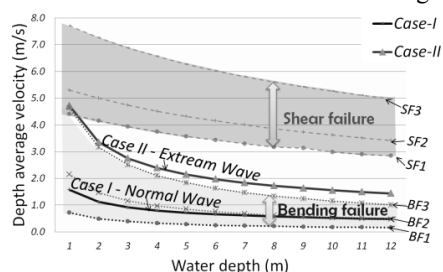


**Fig.6** Comparison of threshold flow velocities (for the bending and shear failure of poles) and velocities for normal (*Case I*) and extreme (*Case II*) wave conditions.

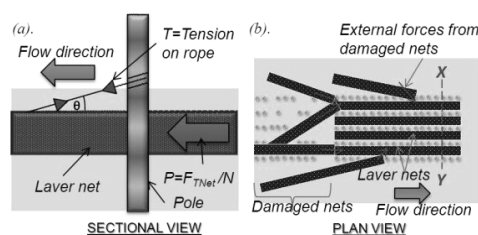


**Fig.7** (a). Tension force on a rope due to equally distributed horizontal force on laver net (b). External effects on a *Nori-Hibi* net from damaged neighboring compartments.

are directly depended on the strength and sectional properties of the bamboo pole

### b) Breakage of ropes

To assess the possibility of breaking the ropes which tie laver nets and supporting poles, maximum tension force acting on a rope was analyzed. For our calculation, total horizontal force ( $F_{TNet}$ ) on a *Nori-Hibi* compartment was equally distributed among all ropes such that to estimate the average tension force developed on a single rope (**Fig. 7 (a)**). Assuming type of rope as Nylon and diameter as 5 mm, its minimum breaking strength was taken as 3.91 kN (Engineeringtoolbox, 2012). Thus, minimum flow velocity required for the tension failure of the ropes was estimated as 5.64 m/s. Compared with the maximum flow velocities of 1.58 m/s in the very highly damaged Futtsu cape area, calculated threshold value for the rope breaking is much higher. However, according to Sasaki *et al.* (2012), some damages due to the rope breaking was recorded in Kaneda in the Banzu tidal flat. Therefore, in addition to the horizontal force that has been exerted by laver nets in the compartment itself, there would be sequential external forces on laver nets due to the flock of *Nori-Hibi* from the outside damaged compartments (**Fig. 7 (b)**). Thus, this convergent force might be sufficient to break the rope under the lower flow velocities, despite the minimum velocity required for a single compartment.

### c) Pulling out of poles

As illustrated in **Fig. 8**, supporting poles could be pulled out either in inclined direction or vertical direction. The prior process is more common and could be resulted due to the failure of bed soil and successively due to the effects of the  $F_Y$  (component of  $F_{Net}$  along the pole). In case of vertical pulling out process, vertical forces such as weight of wet laver net ( $w$ ), buoyancy force ( $b$ ) of submerged laver nets and resistance force such as skin friction on the poles are governing forces. Since laver seeding period starts in December and growing period is up to April, larger quantity of laver might have been collected on laver net at the 2011 tsunami event.

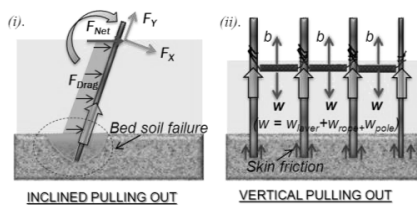


Fig.8 Poles pulling out possibilities.

Therefore, resultant higher laver net ( $F_{Net}$ ) and buoyancy forces ( $b$ ) could have increased the pulling out possibility in both situations.

### (3) Driftage simulation

In this study, initiation of drifting was assumed to occur at the same time at which the *Nori-Hibi* sets were damaged. In failure mode analysis, minimum velocities required for the "breakage of supporting poles" for bending criteria (BF1, BF2 and BF3) were computed for different depth ranges. Thus, threshold parameters corresponding to "breakage of supporting poles" were used as the only failure mode. The failure modes of "breakage of ropes" and "pulling out of poles" which had been discussed based on number of assumptions was not considered for the drifting simulation due to the complexity of the processes. Fig. 9 illustrates the simulated drifting locations for the damaged *Nori-Hibi* sets at  $t = 0$  and 4 hours respectively. According to the simulated results under each criterion, *Nori-Hibi* sets in F area have been shifted up to a significant distance compared to the *Nori-Hibi* sets in B area. It agrees with the damage scales summarized in Table 1. Further, according to the field records, BF1 results are closer to the real damages shown in Table 1. In case of BF2 and BF3 criteria, intensity of damage has been reduced with the stronger bamboo poles. Since these results reflects only the damage effects of supporting poles, higher damages

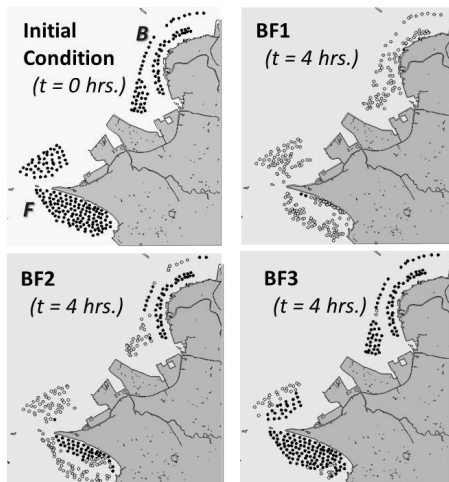


Fig.9 Driftage simulation model results for BF1~BF3 criteria.

could be expected in both areas if simulation could include three failure modes reasonably.

However, on the basis of selected failure criteria and availability of the field information, intensities of damages in the study area are qualitatively explained with driftage simulation model.

## 5. CONCLUSIONS

The magnitude of the calculated total external forces on the *Nori-Hibi* sets, exerted by tsunami flow are in agreement with the damage intensities in the Futtsu cape and Banzu tidal flat areas. Accordingly, a positive correlation was identified between the scales of damages and both external forces (laver net force and drag force along the supporting poles) exerted on *Nori-Hibi* sets. In order to initiate the driftage of the damaged *Nori-Hibi* in driftage simulation model, failure mechanisms were assessed under different failure modes. However, Due to the complexity of other modes, only "breakage of supporting poles" mode was selected for the simulation. In case of breakage of supportive poles, failure was governed by the bending. Further, diameters of bamboo pole and bending strength are identified as important parameters which govern the accuracy of the results.

According to this study, the driftage simulation model has given reasonable results to assess the *Nori-Hibi* sets damages patterns qualitatively. However, it is plausible that a number of limitations and assumptions could have influenced the results obtained.

## REFERENCES

- Borgese, E.M. (1980): *Sea farm: The tory of aquaculture*, Harry N. Abrams, Incorporated, New York.
- Deltaers. (2010): Delft3d-Flow user manual, version 3.14.
- Engineeringtoolbox. (2012): Retrieved June 1, 2012, from [http://www.engineeringtoolbox.com/nylon-rope-strength-d\\_1513.html](http://www.engineeringtoolbox.com/nylon-rope-strength-d_1513.html)
- Janssen, J. J. A. (1981): *Bamboo in Building Structures*, Ph.D. Thesis, The Eindhoven University of Technology, The Netherland.
- Sasaki, J., Ito, K., Suzuki, T., Wiyono, R.U.A., Oda, Y., Takayama, Y., Yokota, K., Furuta, A. and Takagi, H. (2012): Behavior of the 2011 Tohoku earthquake tsunami and resultant damage in Tokyo Bay, *Coastal Engineering Journal*, JSCE, Vol.54, No.1, 26pp.
- Schlichting, H. (1979): *Boundary-Layer Theory*, McGraw Hill, New York, U.S.A.
- Takayama, Y., Ito, K. and Maekawa, K. (2010): Trial Simulation for Behavior of Scallop Larva in Lake Saroma, *Jour. of JSCE, Ser. B2 (Coastal Eng.)*, Vol.66, No.1, pp.1121-1125 (in Japanese).
- Yagi, H., Ishida, H., Takahashi, A., Nadaoka, K., Tamura, H & Kotani, M. (2009): Influence of laver aquaculture facilities on tidal currents and suspended particulate matter transport at the head of Ariake Bay, *Coastal Engineering Journal*, JSCE, Vol. 52, No.3, pp.275-295.

(Received June 15, 2012)